Supplementary Information for:

Fatty Acid Flippase Activity Of UCP2 Is Essential For Its Proton Transport In Mitochondria

Marcelo J. Berardi and James J. Chou

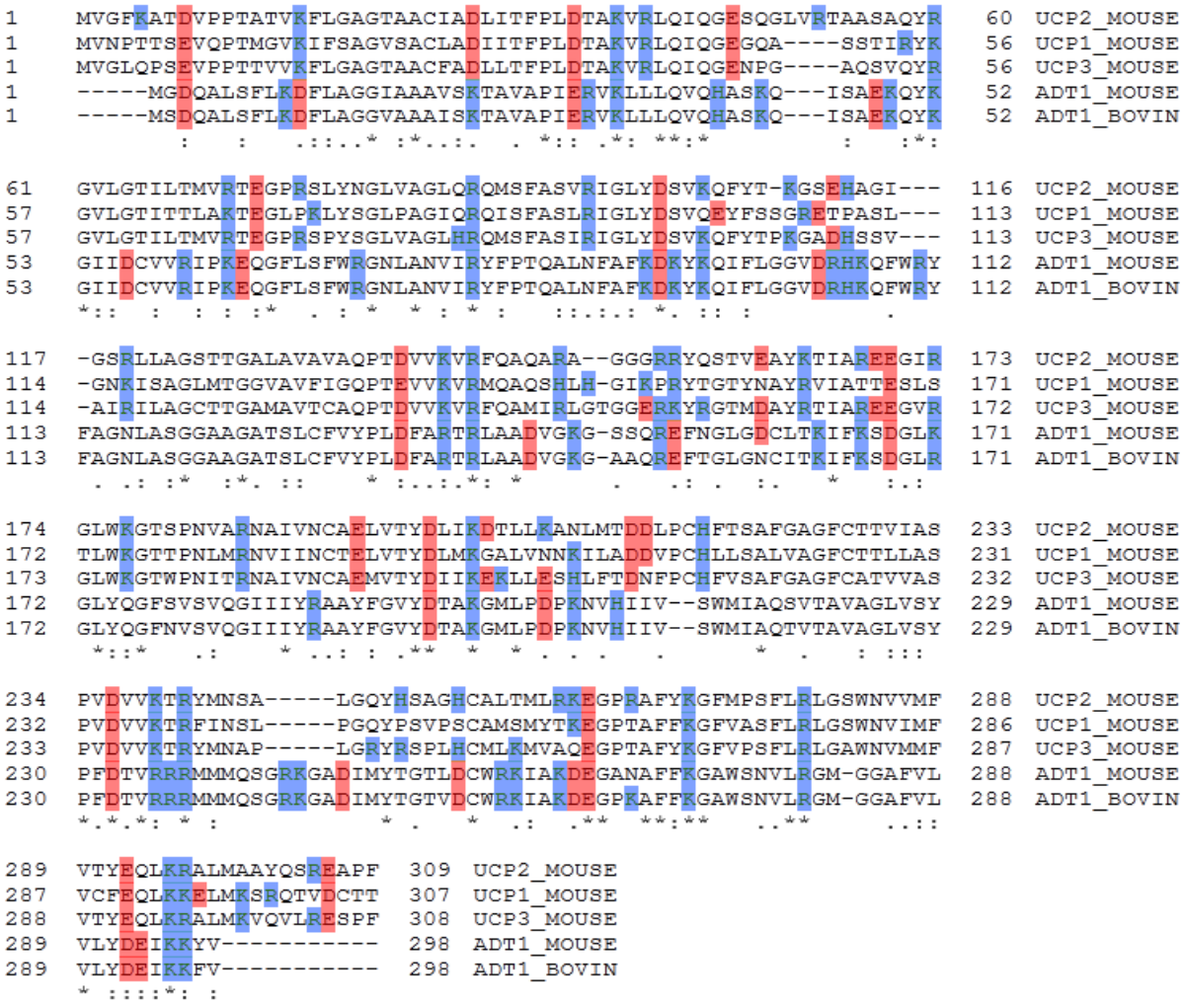

Figure S1. Sequence Similarity Between the UCPs and AACs, related to Figure 1

Sequence alignment of murine UCP2, UCP1, UCP3, AAC (ADT1) and bovine AAC (ADT1) using the Clustal Omega program (Sievers et al., 2011). The symbol '*' indicates positions of fully conserved residues, and ':' and '.' indicate conservation between residues of strongly and weakly similar properties, respectively. Positively and negatively charged residues are shown in blue and red, respectively.

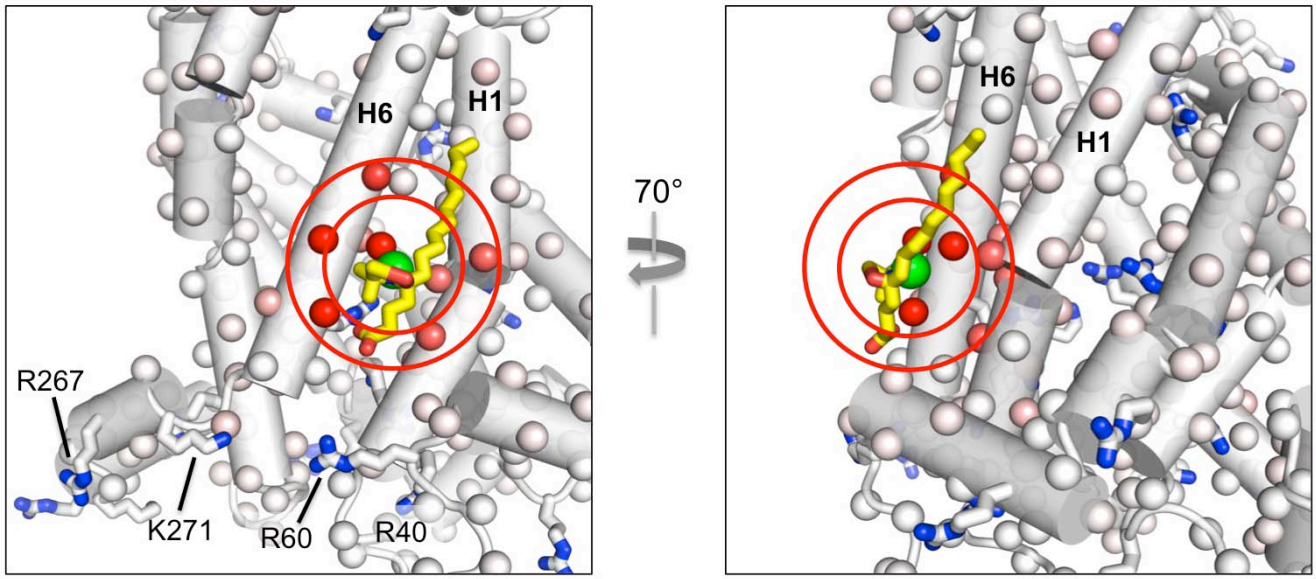

Figure S2. Placement of NO-FA in UCP2 Based on PRE Results, related to Figure 2 and 3

More detailed views of Fig. 2C show the PRE effects (red balls) that are sensitive to GDP titration as well as the sidechains of basic residues. Concentric circles of 1 and 1.5 nm diameters are centered on the modeled position of the O• (green ball) of the nitroxide group of NO-FA (in yellow). The UCP2 model used here is the NMR-derived backbone structure of the GDP-bound UCP2 (PDB code: 2LCK). In this model, NO-FA assumes an orientation such that its acyl chain is partitioned in the hydrophobic core of the detergent micelles.

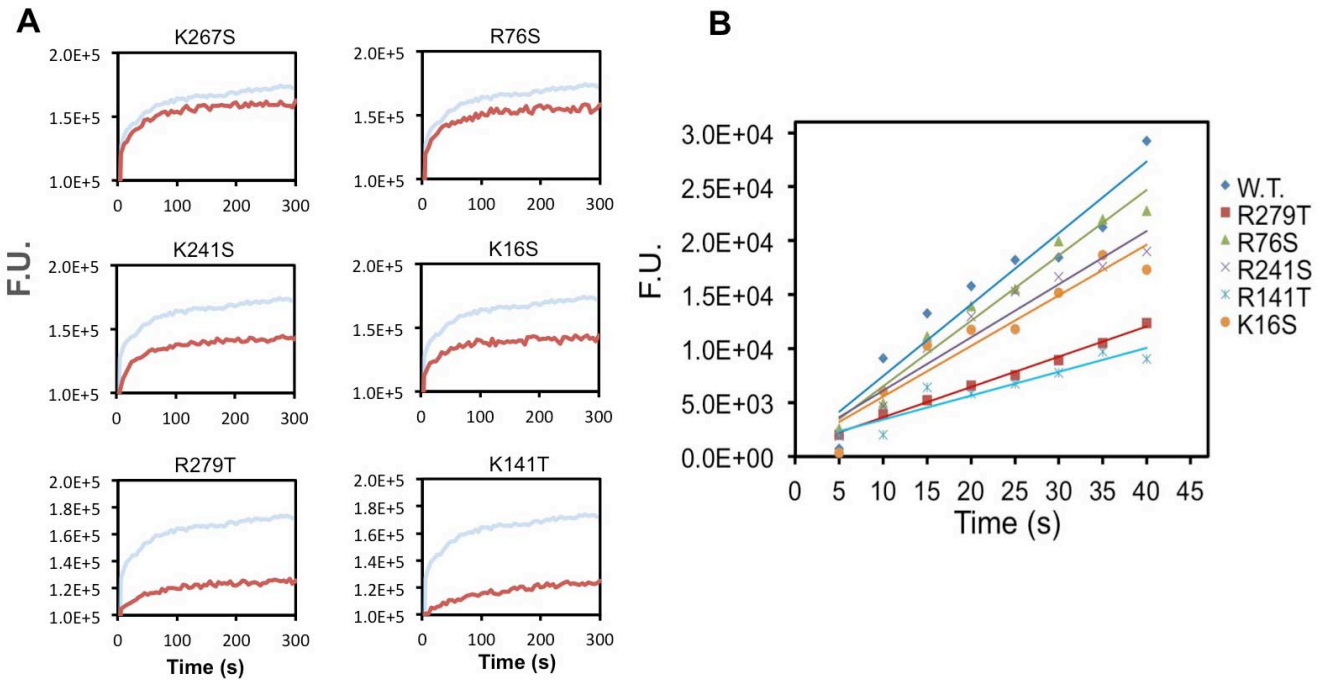

Figure S3. The H^+ Translocation Activities of Additional Mutants, related to Figure 4

(A) Traces in red are the time traces of H^+ efflux of additional UCP2 mutants obtained using the assay in Fig. 4A. The light blue trace corresponds to the WT UCP2, which is included for direct comparison. Single mutations K267S and R276S have no significant effect on H^+ flux whereas K241S, K16S, R279T and K141T show significantly reduced activity.

(**B)** The initial slopes of the traces in (A) for better quantification of the effects of mutations on UCP2 mediated H^+ translocation.

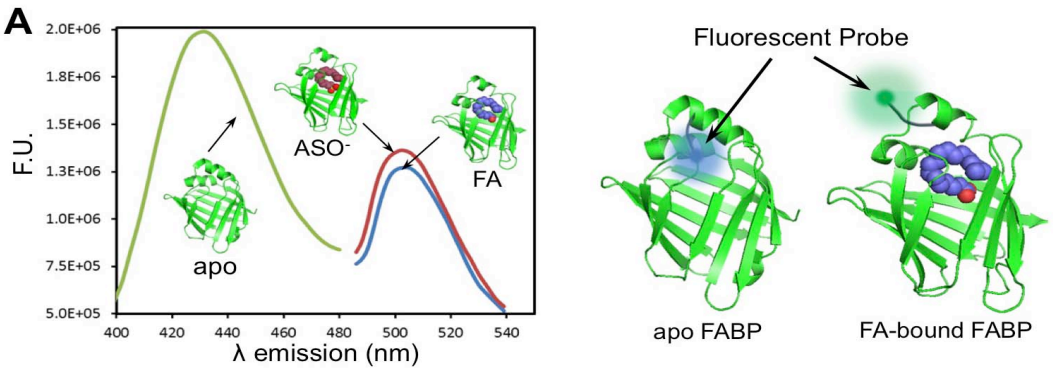
A
F.U.
2.0E+06
1.8E+06
1.5E+06
1.3E+06
1.0E+06
7.5E+05
5.0E+05
400
420
440
460
480
500
520
540
λ emission (nm)
apo
ASO-
FA
Fluorescent Probe
apo FABP
FA-bound FABP

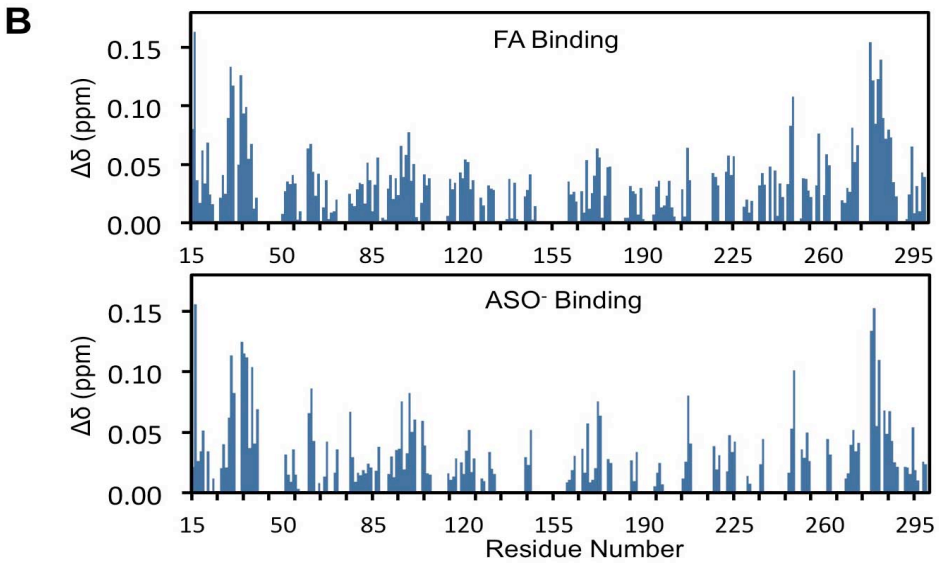
B
FA Binding
ASO- Binding
Δδ (ppm)
0.15
0.10
0.05
0.00
15
50
85
120
155
190
225
260
295
Residue Number

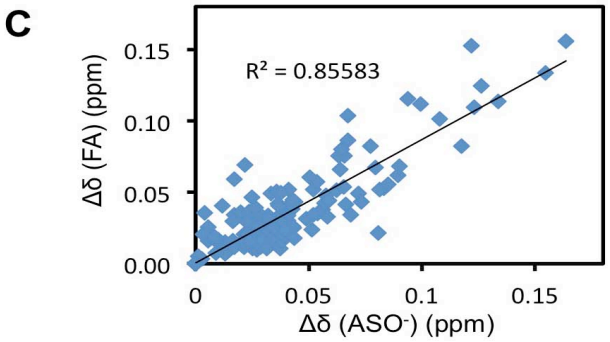
C
R² = 0.85583
Δδ (FA) (ppm)
Δδ (ASO-) (ppm)
0.15
0.10
0.05
0.00
0
0.05
0.1
0.15

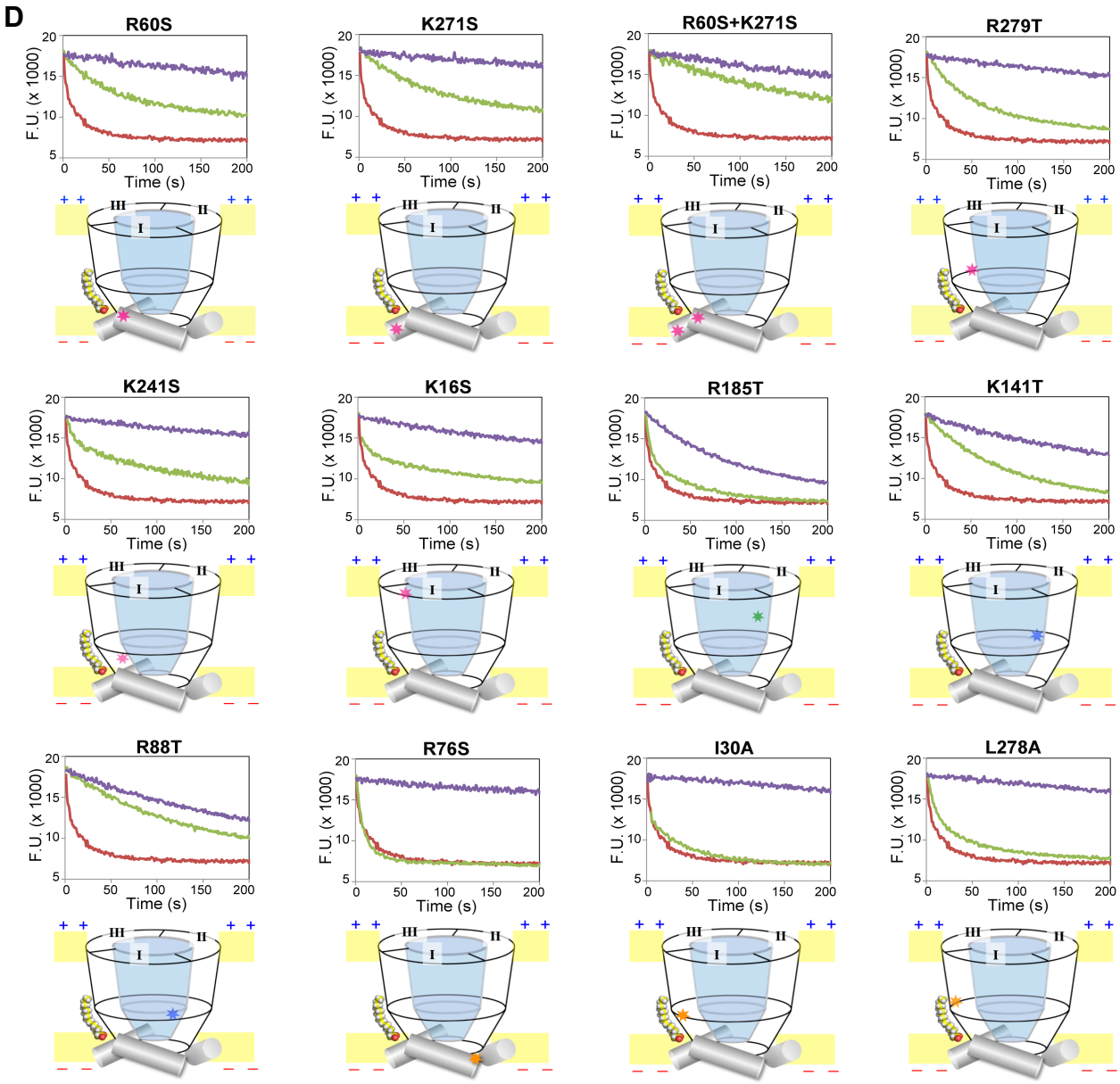

Figure S4. The ASO$^-$ and FA Show Similar Properties of Binding to FABP and UCP2 and Raw Functional Mutagenesis Data, related to Figure 5

(A) FABP fluorescence shift upon FA and ASO$^-$ binding, as shown by emission spectrum of apo FABP (green), FABP in the presence of 50 μM FA (blue), and FABP in the presence of 200 μM ASO$^-$ (red). The excitation wavelength is 380 nm. The right panel illustrates the environmental change of the acrylodan probe (hydrophobic to hydrophilic) upon FA binding.

(B) Residue-specific chemical shift changes of WT UCP2 ($\Delta\delta = [(\omega_H\Delta\delta_H)^2 + (\omega_N\Delta\delta_N)^2 + (\omega_C\Delta\delta_C)^2]^{1/2}$, ω_H = 1.00, ω_N = 0.15, ω_C = 0.35) induced by FA (top panel) and ASO$^-$ (bottom panel).

(**C)** Strong correlation between FA and ASO^- induced residue-specific $\Delta\delta$ in (B) indicates that ASO^- and FA binds to UCP2 in the same way.

(D) Effects of Mutations on UCP2-Catalyzed ASO^- Flipping and Inhibition by GDP. For each of the mutants, the fluorescence traces, for monitoring ASO^- flipping by UCP2 as in Fig. 5, in the absence and presence of 100 μM GDP are shown in green and purple, respectively. The ASO^- flipping activity of the WT UCP2 is shown by the red trace, recorded using the same protein and ASO^- concentration as for the mutants. The locations of the single and double mutations are displayed qualitatively in a cartoon drawing of UCP2 by the stars. The color assignment of the star is: pink – significant reduction of ASO^- flipping but not GDP inhibition; green – significant reduction of GDP inhibition but not ASO^- flipping; blue – affecting both ASO^- flipping and GDP inhibition; orange – affecting neither ASO^- flipping nor GDP inhibition. The traces displayed here are typical traces from three independent measurements.

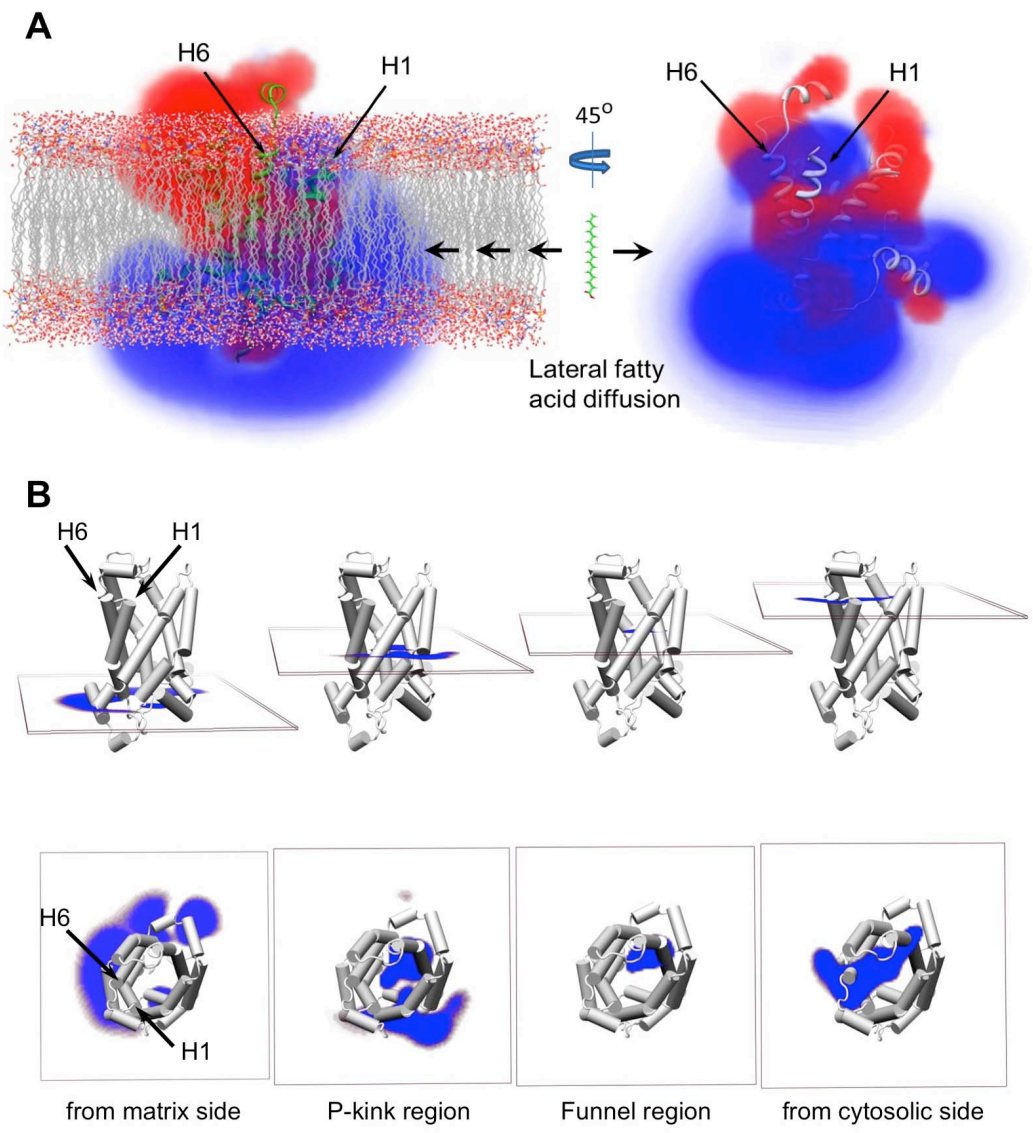

Figure S5. UCP2 Electrostatics and FA Binding, related to Figure 6

(A) The average electrostatic potential of the 15 lowest energy conformers of UCP2 (PDB ID: 2LCK) is represented as a 3D density map. The electrostatic potential was calculated using a finite difference solution to the non-linear form of the Poisson-Boltzmann equation with the program DelPhi (Li et al., 2012). The positive and negative components are shown in blue and red, respectively. The figure suggests that FA partitioning in the lipid bilayer and lateral diffusion allow the negatively charged carboxylate of FA to occupy the blue regions of the electrostatic potential.

(B) Slices of the electrostatic potential parallel to the lipid bilayer showing only the positively charged components at various depth of the UCP2 cavity.